# CHAPTER 117

## WAVE OSCILLATIONS IN AN OFFSHORE OIL STORAGE TANK

By Hooshang Raissi[1]

### INTRODUCTION

The rapidly increasing demand to exploit known offshore oil fields throughout the world, and the costly conventional method of piping the oil to the shore have given support to the concept of offshore storage terminals located in the immediate vicinity of the field. The Khazzan Dubai oil storage tanks at Fateh field, offshore from Dubai (Chamberlin, 1970), the Pazargad one million-bbl crude-oil storage barge at Syrus field, Iran, offshore in the Persian Gulf (Feizy and McDonald, 1972), and the new offshore reinforced-concrete million-bbl oil storage tank at the Ekofisk field in the North Sea (Ocean Industry, 1972), show the new attitude which the offshore oil-production industry has developed toward this system.

A closed floating, or pile-supported, bottomless barrier might provide an effective solution for storing oil offshore or containing an oil spill.

The crude oil coming from the production platform is injected at the sea level inside the closed bottomless barrier, it dispalces the water inside, and remains above the water as a result of its density. The oscillations of the internal wave at the interface of oil and water and the surface waves resulting from different incident waves in such a container were studied in this work.

### THEORETICAL ANALYSIS

Suppose that a homogenous layer of fluid of density $\rho_1$ (oil) of thickness h lies over another homogeneous layer of fluid of density $\rho_2$ (water) of thickness H-h (see Fig. 1). The two fluids are immiscible, and the surface tension and viscosity of the fluids will not be taken into account.

---

1- Assistant Professor University of Tehran - Iran

The boundary conditions at the interface are as follows:

a. Vertical velocity is the same in both fluids:

$$\Phi_{1Z}=\Phi_{2Z}=\eta_{2Z} \quad \text{at} \quad Z=+h \tag{1}$$

b. Pressure is continuous at the interface:

$$P_1=\rho_1\left(\Phi_{1t}+g(h-\eta_2)\right)$$

$$P_2=\rho_2\left(\Phi_{2t}+g(h-\eta_2)\right)$$

so that

$$\rho_2\left(\Phi_{2t}+g(h-\eta_2)\right)=\rho_2\left(\Phi_{1t}+g(h-\eta_2)\right) \tag{2}$$

Taking the partial derivative of Eq. (2) with respect to t gives

$$\rho_2\Phi_{2tt}-\rho_1\Phi_{1tt}-g(\rho_2-\rho_1)\,\eta_{2t}=0 \tag{3}$$

The free-surface boundary condition is

$$\Phi_{1tt}+g\,\Phi_{1z}=0 \quad \text{at} \quad Z=0 \tag{4}$$

The bottom boundary condition is

$$\Phi_{2Z}=0 \quad \text{at} \quad Z=H \tag{5}$$

From the continuity equation for an incompressible fluid, $\vec{\nabla} U = 0$, and the definition of the velocity potential, Laplace's equation is obtained:

$$\nabla^2\Phi_1=0 \tag{6}$$

$$\nabla^2\Phi_2=0 \tag{7}$$

Therefore, the problem is to find the velocity potentials $\Phi_1$ , and $\Phi_2$ , which satisfy Laplace's equations, Eqs. (6) and (7), subject to a number of prescribed boundary conditions. Using the method of separation of variables, we will get to the following equation, (wehausen 1970).

$$\frac{\sigma^2}{gk} = \frac{\rho_2(\coth kh+1) \pm \{\rho_2(\coth kh-1)+2\rho_1\}}{2\{\rho_2 \coth kh + \rho_1\}} \tag{8}$$

for(+)

$$\frac{\sigma^2}{gk} = 1.0 \tag{9}$$

for(-)

$$\frac{\sigma^2}{gk} = \frac{\rho_2 - \rho_1}{\rho_2 \coth kh+\rho_1} \tag{10}$$

From Eq. (g) we have

$$\eta_1 = (a \operatorname{Cos}kx + b \operatorname{Sin}kk) \operatorname{Sin} (\sigma t + \tau) \tag{11}$$

$$\eta_2 = e^{-kh}(a \operatorname{Cos}kx + b \operatorname{Sin}kx) \operatorname{Sin} (\sigma t + \tau) \tag{12}$$

and from Eq. (10) we have

$$\eta_1 = (a \operatorname{Cos}kx + b \operatorname{Sin}kx) \operatorname{Sin} (\sigma t + \tau) \tag{13}$$

and

$$\eta_2 = \frac{\rho_1}{\rho_2 - \rho_1} e^{kh} (a \operatorname{Cos}kx + b \operatorname{Sin}kx) \operatorname{Sin} (\sigma t+\tau) \tag{14}$$

Two-Dimensional Case (A Rectangular Bottomless Container)

For the case of two barriers extending from the surface to a given depth ( D ) , assuming that the depth of immersion of the barriers are bigger than half of the surface wavelength. In order to have a resonance motion within the container, we must have

$$\frac{nL}{2} = B \tag{15}$$

where n is the number of half-wavelengths, and B is the distance between the barriers. From Eq.(15),

$$K = \frac{\pi n}{B}$$

Then Eq. (9) becomes:

$$\frac{\sigma^2 B}{\pi g} = n \tag{16}$$

and

$$\eta_1 = A \cos \frac{\pi n}{B} \sin(\sigma t + \tau)$$

$$\eta_2 = A e^{-kh} \cos \frac{\pi n}{B} \sin(\sigma t + \tau)$$

Then Eq (10) becomes:

$$\frac{\sigma^2 B}{\pi g} = n \frac{1 - \frac{\rho_1}{\rho_2}}{\coth \frac{\pi n h}{B} + \frac{\rho_1}{\rho_2}} \tag{17}$$

and

$$\eta_1 = A \cos \frac{\pi n}{B} \sin(\sigma t + \tau)$$

$$\eta_2 = - A \frac{\rho_1}{\rho_2 - \rho_1} e^{kh} \cos \frac{\pi n}{B} \sin(\sigma t + \tau)$$

There will be resonance with a large surface wave whenever

$$\frac{\sigma^2 B}{\pi g} = 1,2,3..... \tag{18}$$

There will be resonance with a large internal wave whenever

$$\frac{\sigma^2 B}{\pi g} = \frac{1 - \frac{\rho_1}{\rho_2}}{\coth\frac{\pi h}{B} + \frac{\rho_1}{\rho_2}},\ 2\,\frac{1 - \frac{\rho_1}{\rho_2}}{\coth\frac{2\pi h}{B} + \frac{\rho_1}{\rho_2}} + ,..., \tag{19}$$

This is not the exact solution of the problem, because the barriers were assumed to extend to a depth which is more than half a surface wave length and also the water depth H was considered to be infinite. For this reason the experimental wave height of the internal waves and surface waves were compared with the numerical solution of this problem, Based on a varitional form of the equation for steady oscillatory irrotational motion of an inviscid incompressible fluid (Bai, 1972).

Three-Dimensional Case (Circular Bottomless Container)

The amplitude variation in polar coordinates in the case of oscillation in a circular basin of constant depth is described by the following expression (Lamb, 1932):

$$\eta = \Sigma_m C_m J_m (Kr) \cos m\theta \cos \sigma t \tag{20}$$

For oscillation inside a cylinder, the following boundary condition should be satisfied:

$$\frac{\partial \eta}{\partial r} = 0 \quad \text{at} \quad r = a \tag{21}$$

(periphery of basin)

This is identical to stating that the normal velocity at the boundary is zero, from Eq.

$$J_m'(Ka) = 0 \tag{22}$$

This means a maximum or a minimum (a crest or a trough) should exist at the outer edge of the cylinder.

The lowest symmetrical mode of oscillation is the first root of $J_0(Ka)$ $\quad Ka = 3.832$

This gives one nodal circle located at $r/a = 0.688$.

The period of the wave which causes this mode of oscillation at the interface of oil and water can be obtained by substituting Eq. (22) into Eq. (10). This gives:

$$\frac{\sigma^2 R}{g} = 3.832 \frac{1 - \frac{\rho_1}{\rho_2}}{\coth(3.832 \frac{h}{a}) + \frac{\rho_1}{\rho_2}} \tag{23}$$

The condition for the same mode of oscillation to occur at the surface of the oil can be obtained by substituting Eq. (22) into Eq. (9), giving

$$\frac{\sigma^2 a}{g} = 3.832 \tag{24}$$

The same calculation is being carried for other modes of osciliation.

## EXPERIMENTAL EQUIPMENT AND ARRANGEMENTS

### Two-Dimensional Model

The two-dimensional model studies were performed in a wave channel that is 1 ft. wide by 3 ft. deep by 100 ft. long (Fig 5).

At one end of the channel there is a flapper-type generator; at the other end a beach was installed to absorb wave energy and minimize wave reflection. Also shown in the figure is a wave filter located in front of the wave machine. A rectangular bottomless container 1 ft. wide by 1.5 ft. deep by 2.33 ft. long was constructed of 1/4 inch lucite, simulating a perfectly reflecting rigid barrier.

Two types of wave gages were used to measure the wave amplitude, one for the internal waves at interface of oil and water, and the other for measuring the surface oil waves inside the container.

For the first type, parallel-wire resistance wave gages were used (Wiegel, 1953). Since oil is a very poor electric conductor compared with tap water only the depth of the immersion of wires in water is proportional to the probe conductivity.

For measuring the surface oil waves inside the container, a capacitance type wave recorder was used . The capacitor has a definite initial capacitance which depends on the probe length, distance between the probes, and the dielectric of the material between the capacitor "plates".

In addition, motion pictures were taken through the glass walls of the channel (while the container had oil inside) of several experimental runs. The camera was mounted so that its line of sight was perpendicular to the side of the flume and level with the undisturbed oil and water interface. A grid on the glass wall of the wave channel, permitted the measurement of the surface and internal waves inside the containers.

Three-Dimensional Modle

This experiment was conducted in an ripple-tank. The tank is 20 feet long, 49½ inches wide, and 4 inches deep. Periodic waves were generated by a mechanical wave flap driven by an electric motor (Fig. 6).

A wave filter was located in front of the wave generator, and circualr Lucite cylinder was used as a model of a circualr oil container.

A section of the bottom ot the ripple tank was made of plate glass, underneath the glass bottom was a plane mirror mounted at 45 degrees to the horizontal. A strong light source was reflected by the mirror through the glass bottom. The light beams were converged by wave crests and diverged by wave troughs. This permitted visual observations of the wave patterns on a horizontally mounted tracing-paper screen above the tank. Pictures were taken of the wave patterns inside the cylinder at different incident-wave conditions by a camera located above the tracing-paper screen (Fig.1).

## PRESENTATION AND DISCUSSION OF RESULTS

Two-Dimensional Model Study

Experimental studies were conducted to measure the periods of waves causing oscillations at the interface of oil and water, and also at the surface of the water.

Measurements were also made of the distribution of maximum internal and surface-wave amplitudes, inside the two-dimensional oil container. Three different liquids with specific gravities of $S = 0.685$, and 0.830 and 0.910 were used to substitute for oil inside the model. The experiments were run for only one depth, $H = 1.5$ ft., and one immersion depth of the barriers, $D = 0.5$ ft. An oil layer of thickness $h = 0.3$ was used inside the oil container (Fig. 1) for all the experiments.

The theoretical solution described in Theoretical Section Eqs. (18 and 19) was used to predict the frequencies associated with surface and internal wave oscillations. Figures 2 to 4 illustrate the theoretical and experimental valuse of $\sigma^2 B/\pi g$ for any mode of surface - and internal-wave oscillation.

Although the mathematical treatment was carried out under the assumption that the depths of the immersion of the barriers are larger than 1/2 the surface wavelength ($D \geqslant 1/2\ L$), the experimental results correspond very well with the theory for all ranges of wave periods ($T = 3.8$ to $0.65$ sec.).

A small difference could be detected between the theoretical values of circular wave frequency and the experimental ones for the surface-wave oscillations. The experimental values were higher than the theoretical ones, especially for the first mode of oscillation which is associated with longer waves. This difference is due to the change in wave number associated with surface wave oscillation caused by insufficient immersion depth of barriers, which makes the theoretical solution only approximate.

However, this effect is not important for higher modes of surface oscillations and internal-wave oscillations owing to the short wave lengths causing them. In this case the theoretical assumption $D \geqslant 1/2\ L$ is valid.

Comparison of Figs. 2 , 3 and 4 show that the change in oil density does not have any significant effect on the period of waves causing the oil-surface oscillations, but that it has a significant effect on the wave periods causing the internal-wave oscillations. The greater the density of the oil, the larger the wave period corresponding to any mode of oscillation.

The computer numerical technique (Bai, 1972), was used to calculate Amplification Factors for comparison with the experimental measurements, (Figs 7 and 8).. The amplification factor (A) for the surface waves is the ratio of the maximum wave height to the incident-wave height, and for the internal waves it is the ratio of the maximum internal-wave height to the incident-wave height. The experimental results for the internal waves agree well with the theory. However, the experiment results show a higher amplification factor for the surface wave than is predicted by theory. This might be due to an insufficient number of internal boundary segments being used along the interface of oil and water for the numerical calculations. An effect of the oil density on the internal - and surface-wave heights during the oscillations could be seen by comparing Figs. 7 and 8. Both show the internal - and surface-wave heights for the first mode of internal-wave oscillation. The internal-wave heights for oil with a density of 0.83 $gr/cm^3$ are higher than the ones for oil with a density of 0.685 $gr/cm^3$.

It should be noted that the incident waves that cause oscillations of the higher-density oil are the longer waves, and that the higher internal-wave oscillations are partially due to the higher wave energy which can penetrate inside the bottomless storage tank. Figure 7 also shows a lower surface-wave height for oil with higher density for the first mode of internal-wave oscillation. This might be due to the fact that the wave period causing the first mode of internal-wave oscillation for oil with lower density, is nearer to the zero mode of oscillation of the surface wave.

Three-Dimensional Study

This experiment was conducted for a water depth of H =3.5 in. The immersion depth of the one-foot diameter circualr oil container was D = 3 in. An oil layer thickness of h = 1in. was used inside the oil container. Figure 11 shows photographes taken of the different modes of oscillation at the interface of the water and oil with an oil density of 0.80 gr/cm$^3$. The theoretical solution Eqs.(23 and 24) predicts the frequencies associated with any mode of surface - and internal-wave oscillation.

Figures 9 and 10 show the theoretical and experimental values of $\sigma^2$ D/g for any mode of internal - and surface-wave oscillation.

## CONCLUSIONS

From the study the following major conclusions are drawn:

1. The prediction from the theory of resonant frequencies for internal and surface waves corresponds very well with the experimental results.

2. A change in oil density does not have any significant effect on the period of the waves need to cause surface-wave oscillation. It does have a significant effect on the period of the waves needed to cause internal-wave oscillation; the higher the density of oil, the higher the wave period needed to generate a particualr mode of oscillation.

3. The experimental results for the internal-wave amplification factors correspond closely to the numerical results. However, the experimental results give higher amplification factors than the theory for the surface waves within the tank.

4. The internal-wave heights are higher for oils with higher density, all other conditions being equal.

ACKNOWLEDGMENTS

The author wishes to express his sincere appreciation to professors R.L. Wieged, J.V. Wehausen and J.W. Johnson for their help and advise throughout this research. Dr. June Bai is acknowledge for his computer program which was used in this work.

The work reported herein was partially supported by the coastal Engineering Research center, corps of Engineers, U.S. Army. It was also partially supported by the Sea Grant Program at the university of Calaifornia.

REFERENCES

1. Bai, Kwang, June, "A Variational Method in Potentail Flows with a Free Surface, "Ph.D. Thesis in Naval Architecture, University of California, Berkeley, California, 1972.

2. Chamberlin, R. S., "Khazzan Dubai, Design, Construction and Installation, "Chicago Bridge and Iron Co. Paper No. OTC 1492, Preceedings of Second Offshore Technology Conference, Dallas, Texas, April 1970.

3. Feizy, G., and McDonald, J. E., "Pazargad-World's Largest Crude Oil Storage Barge, "Iran Pan American Oil Co. Paper No. OTC 1526, Proceedings of Fourth Offshore Technology Conference, Houston, Texas, May 1972.

4. Lamb, H., Hydrodynamics, Sixth Edition, Dover Publications, New York, 1945.

5. Ocean Industry, "North Sea Report, "Phillips Ekofisk Million Barrel Oil Storage Tank Near Completion, PP. 33-35, July 1972.

6. Wiegel, Robert, Parallel Wire Resistance Wave Meter, Coastal Engineering Instruments, Council on Wave Research, The Engineering Foundation, 1953, PP. 39-43.

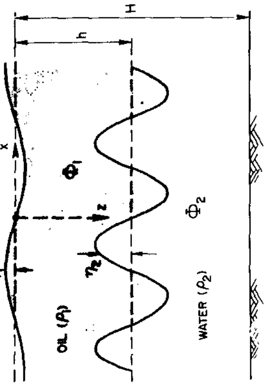


FIG. 1 DEFINITION SKETCH OF OIL-WATER COORDINATE SYSTEM

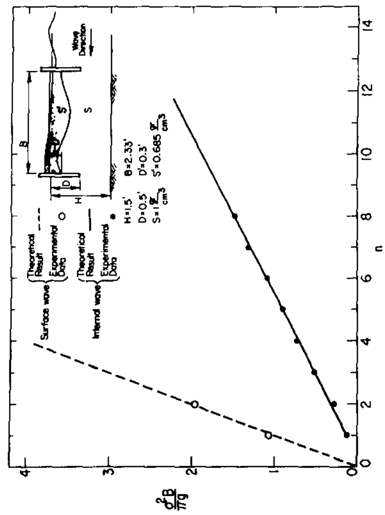


FIG. 2 THEORETICAL AND EXPERIMENTAL VALUES OF $\left(\frac{\sigma^2 B}{\pi g}\right)$ FOR ANY MODE OF OSCILLATION

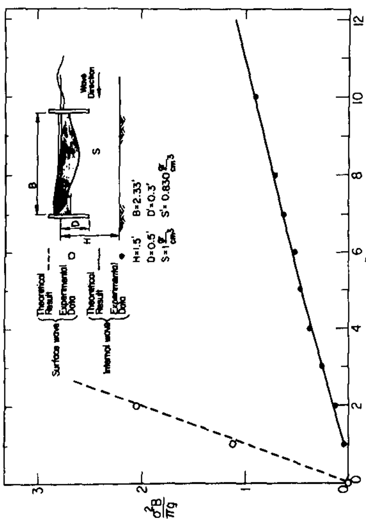


FIG. 3 THEORETICAL AND EXPERIMENTAL VALUES OF $\left(\frac{\sigma^2 B}{\pi g}\right)$ FOR ANY MODE OF OSCILLATION

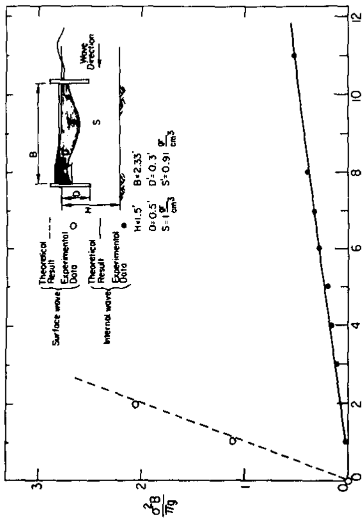


FIG. 4 THEORETICAL AND EXPERIMENTAL VALUES OF $\left(\frac{\sigma^2 B}{\pi g}\right)$ FOR ANY MODE OF OSCILLATION

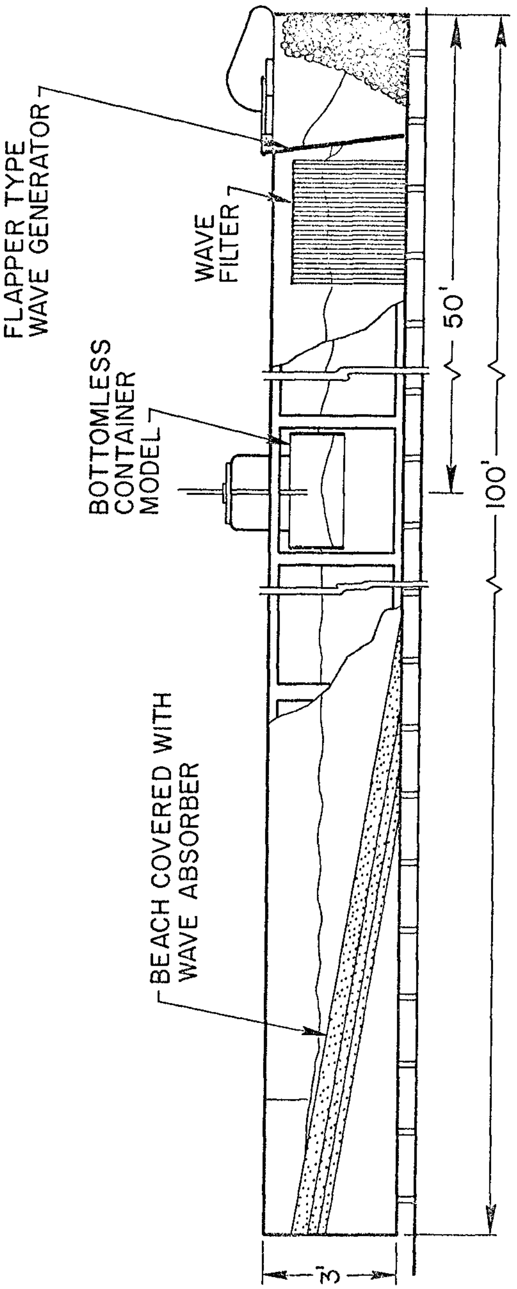


FIG. 5 DRAWING OF THE WAVE CHANNEL

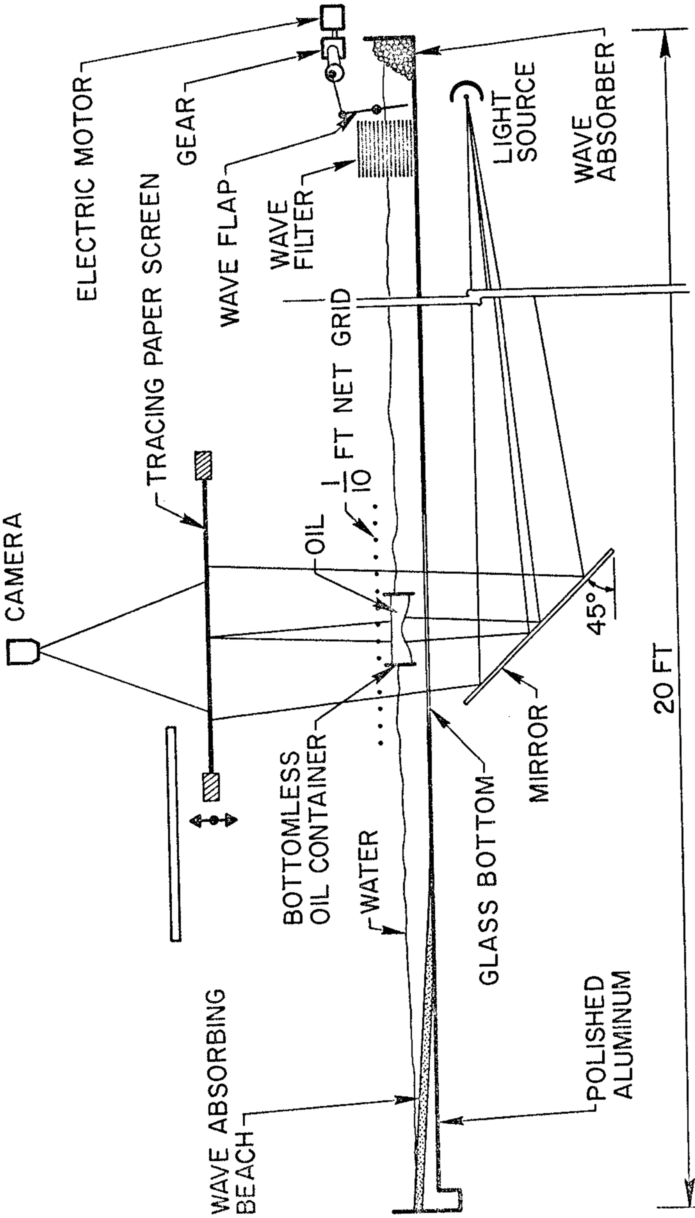


FIG. 6 THE RIPPLE TANK

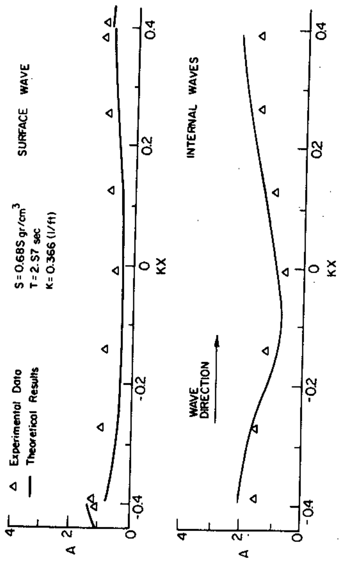


FIG. 7 MAXIMUM WAVE AMPLITUDES OF INTERNAL AND SURFACE WAVES

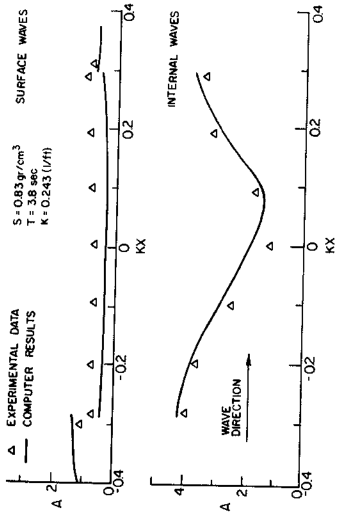


FIG. 8 MAXIMUM WAVE AMPLITUDES OF INTERNAL AND SURFACE WAVES

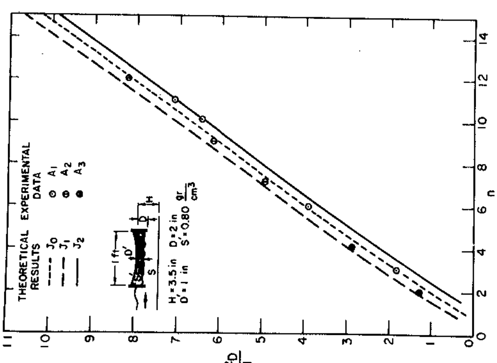


FIG. 9 INTERNAL WAVE OSCILLATION

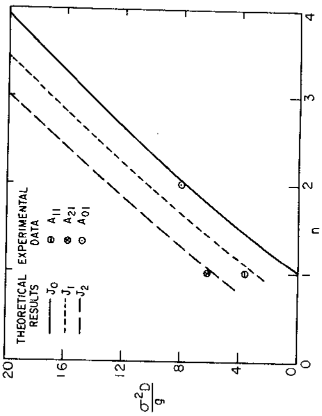


FIG. 10 SURFACE WAVE OSCILLATION

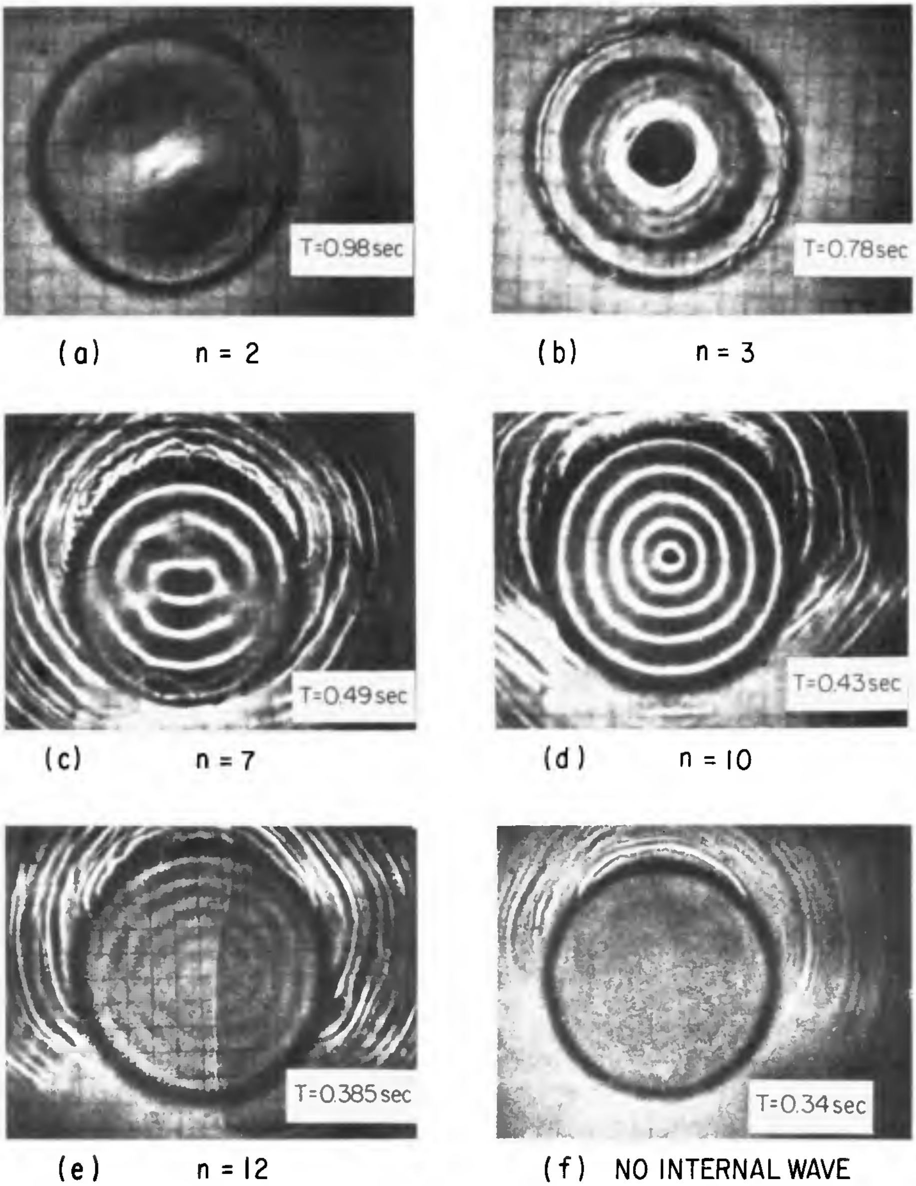


FIG. 11 INTERNAL WAVE PATTERN INSIDE THE CIRCULAR BOTTOMLESS OIL CONTAINER